

Circularly Polarized Light Standards for Investigations of Collagen Fiber Orientation in Bone

TIMOTHY G. BROMAGE,* HAVIVA M. GOLDMAN, SHANNON C. McFARLIN, JOHANNA WARSHAW, ALAN BOYDE, AND CHRISTOPHER M. RIGGS

Bone exhibits positive form birefringence dominated by and dependent upon the orientation of its collagen. The biomechanical efficacy of bone as a tissue is largely determined by collagen fibers of preferred orientation and distribution (and corresponding orientation of mineral crystallites), and evidence is accumulating to demonstrate that this efficacy extends to function at the organ level. This study has three aims. The first is to provide a background to the study of circularly polarized light (CPL) investigations of collagen fiber orientation in bone. The significance of preferred collagen fiber orientation in bone, linearly polarized light and CPL imaging principles, and a short history of CPL studies of mammalian functional histology are reviewed. The second is to describe, in some detail, methodological considerations relating to specimen preparation and imaging appropriate for the quantitative analysis of preferentially oriented collagen. These include section transparency, section thickness, the uniformity of the illuminating system, and CPL paraphernalia. Finally, we describe a grey-level standard useful for quantitative CPL, based upon mineralized turkey tendon, which shall be provided to investigators upon request. When due consideration is paid to specimen preparation and imaging conditions, quantitative assessment of collagen fiber orientation provides insight into the effects of mechanical loading on the skeleton. *Anat Rec (Part B: New Anat)* 274B: 157-168, 2003. © 2003 Wiley-Liss, Inc.

KEY WORDS: circularly polarized light; collagen; bone; imaging

Dr. Bromage, Ms. McFarlin, and Ms. Warshaw are at the City University of New York and the New York Consortium in Evolutionary Primatology. Dr. Goldman is in the Department of Neurobiology and Anatomy, Drexel University College of Medicine. Dr. Boyde is in the Department of Anatomy and Developmental Biology, University College London. Dr. Riggs is in the Veterinary Clinical Services, The Hong Kong Jockey Club, Equine Hospital, Hong Kong SAR, China. The authors are mineralized tissue biologists engaged in an eclectic range of comparative investigations of interest to the biological, anthropological, medical, paleontological, and veterinary sciences. They regard the development of practical solutions to technical problems of specimen preparation and imaging as an essential responsibility and contribution to the field. *Correspondence to: Timothy G. Bromage, Hard Tissue Research Unit, Hunter College of the City University of New York, New York, NY 10021. Fax: 212-772-5419; E-mail: tbromage@hunter.cuny.edu

DOI 10.1002/ar.b.10031
Published online in Wiley InterScience
(www.interscience.wiley.com).

INTRODUCTION

Studies of skeletal functional adaptation and morphology have largely focused on the study of bone at the organ level. Recently, an appreciation for the influence of mechanical loading on bone microstructure has motivated researchers to investigate aspects of a bone's material and structural properties at levels below the macroscopic, in combination with skeletal macroscopic structure. Among those micromorphological features of bone tissues that may be useful for comparative skeletal analysis are those that influence the mechanical properties of bone and that can be modified by physiological processes in response to mechanical loading. The preferred orientation of collagen fibers in bone is one such feature. Here, we wish to concentrate on the method and analysis of preferentially oriented collagen in bone as relevant to studies of the

functional micromorphology of non-human primate and human bone.

BACKGROUND

Preferred Collagen Fiber Orientation

The hypothesis that collagen fibers of preferred orientation and distribution have biomechanical significance was first set forth by Gebhardt (1905) and later tested by Ascenzi and Bonucci (1964, 1967, 1968) and Simkin and Robin (1974). These authors provided evidence that collagen fibers and mineral crystallites in a predominantly transverse orientation, perpendicular to the long axis of the bone, are better able to resist compressive forces, whereas longitudinal fibers and crystallites, oriented more parallel to the long axis of the bone, are better able to resist tensile forces. Collagen fibers oriented at 45 degrees between longitudinal and transverse lamellae were

Box 1: Polarized Light Microscopy of Bone

Polarized light. Polarized light microscopy provides unique information about the structure and composition of a variety of organic and inorganic materials that is not available with other techniques. Here, we briefly describe linearly polarized light (LPL) principles.

The behavior of light can be modeled according to its wave-like properties. Electromagnetic fields oscillate in planes perpendicular to the direction of light propagation, with all vibration planes being equally probable (i.e., unpolarized; see Figure 2 in main text). When the light is linear- or plane-polarized with an arrangement of two polarizing filters, one vibration direction is isolated. The first filter (termed the polarizer) is positioned between the light source and the specimen, permitting light to pass in only one vibration direction, its transmission axis. The second filter (termed the analyzer) is positioned between the specimen plane and the observer (i.e. the eyepiece objectives or re-

ording system), with its vibration direction at 90 degrees to that of the polarizer. In the absence of a birefringent material (see below) in the optical path, the analyzer blocks all light emanating from the polarizer: The image therefore appears black, or extinct. When a birefringent specimen is placed between the two filters, the optical properties of that material interact with light exiting the polarizer to change its vibration direction to that of the analyzer such that the light may pass.

Circularly polarized light (CPL; described further in the text and illustrated in Figure 2) differs from linearly polarized light (LPL) as described above by having an arrangement of filters that allows refracted light emerging from a birefringent specimen in all 360 degrees of arc to be polarized along the transmission axis of the analyzer (Figure 2).

Bone material anisotropy and birefringence. Birefringent materials display optical anisotropy when

viewed by polarized light. This anisotropy is expressed as variation in brightness determined by differences in light refraction by the material. Such variations are direction dependent; they reflect differences in the orientation of crystallographic axes within the material. Collagen is an anisotropic material. When collagen fibers are aligned perfectly transverse to the direction of the light propagation, there is a change in the refraction of light exiting the specimen, resulting in maximum brightness. When collagen fibers are aligned along the axis of light propagation, no refraction occurs and the specimen appears dark, or extinct. Collagen fibers oriented in other directions result in intermediate brightness values. In most cases, embedding (e.g. PMMA) and mounting media may be ignored as influencing the light propagation, as their average contribution to the refractive index is very near to that of microscope glass slides and coverslips (i.e., ca. 1.515 to 1.520).

said to provide better resistance to shear (Ascenzi and Benvenuti, 1986). Collagen fibers of differing orientation can be visualized in polarized light, so that collagen fibers oriented transversely appear bright, those oriented longitudinally appear dark, and fibers having intermediate orientations appear in different levels of grey. (Please refer to Box 1 for a discussion of the properties of polarized light.)

To date, investigations of collagen fiber orientation in bone have tended to focus on secondarily remodeled bone and, with a few exceptions (Mason et al., 1995; McMahon et al., 1995; Riggs et al., 1993a; Simkin and Robin, 1974), primary bone tissues remain relatively unexplored in this respect. Three representative patterns of lamellar organization within secondary osteons have been described by Ascenzi and Bonnucci (1968). Figure 1a illustrates examples of all three types. According to this classification, a Type I osteon consists of lamellae containing collagen fibers coursing in a primarily transverse orientation to the osteon axis. In a Type II osteon, suc-

Our interest in the study of lamellar bone structure focuses on how it reflects the mechanical demands made upon bone in life.

cessive lamellae alternate between longitudinally and transversely oriented collagen fibers. A Type III osteon consists of lamellae containing collagen fibers coursing in a primarily longitudinal orientation parallel with the osteon axis.

Recent studies have recognized that the classification of osteonal architectures as presented by Ascenzi and Bonnucci (1968) must be revamped and is being revisited (Rho et al., 1998). For instance, Giraud-Guille (1988) observes a rotating plywood-like architecture of the collagen fibrils in examined lamellae. Marotti (1993)

indicates that the homogeneity of fibrillar orientation depends upon lamellar thickness. Ascenzi et al. (2003) provide evidence that dark lamellae are dominantly composed of collagen fibers parallel with the osteon axis (corroborating the traditional view), whereas bright lamellae vary in their fiber orientation, some lying at transverse orientations but most having collagen oriented ± 45 degrees about the osteon axis.

Our interest in the study of lamellar bone structure focuses on how it reflects the mechanical demands made upon bone in life. From this perspective, although revisionist theories are important for interpretations of lamellar organization, at present, there are no contradictions to the general hypothesis that variability in brightness as observed by polarized light microscopy of bone is related to variability in the overall preferred orientation of the collagen fibers within lamellae. Further to this, investigators to date (e.g., those cited below in relation to various mammalian taxa) have assumed that brightness, as observed by

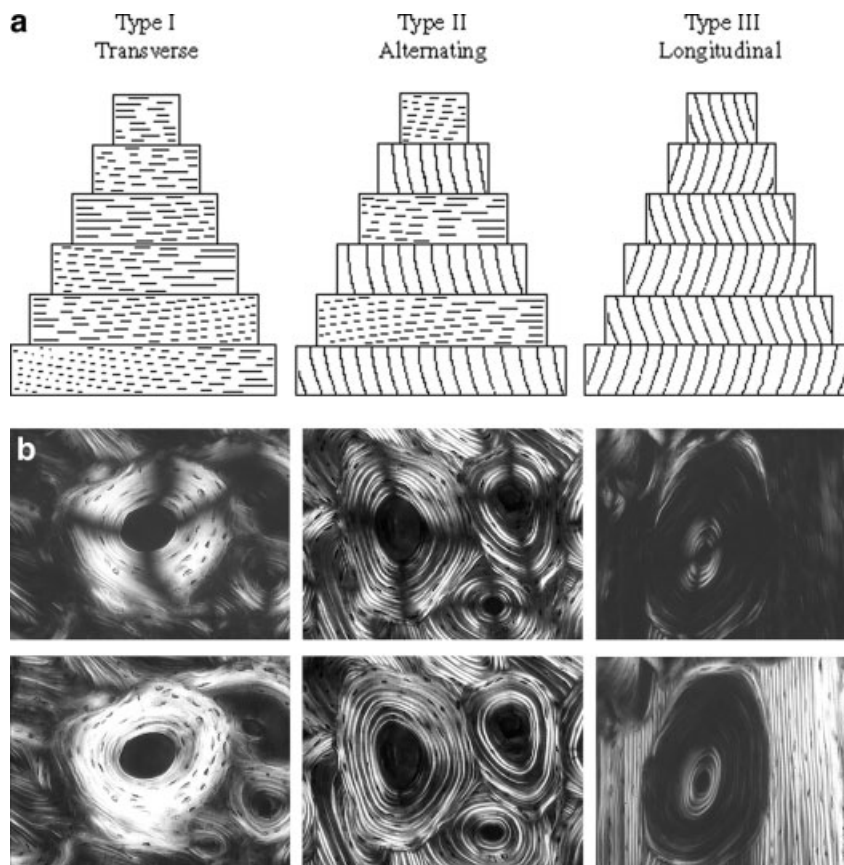


Figure 1. a: Secondary remodeling events, or osteons, may be generated along a continuum of lamellar organization representing extremes of collagen fiber orientation (horizontal and vertical hatching). Concentric lamellae are represented from the innermost (top) to the outermost (bottom) lamella. Figure adapted from Ascenzi and Bonnucci (1968). **b:** Top row: linearly polarized light (LPL) images. Bottom row: circularly polarized light (CPL) images. Left: Transverse osteons contain lamellae composed of collagen fibers transverse to the osteon axis and are bright in CPL. Middle: Alternating osteons contain lamellae composed of collagen fibers that alternate between transverse and longitudinal to the osteon axis, and which are bright and dark in CPL, respectively. Right: Longitudinal osteons contain lamellae composed of collagen fibers parallel with the osteon axis and are dark in CPL. Note artifactual extinction in the form of a Maltese Cross in LPL images of bright lamellae (top row) in comparison to light transmittance in CPL (bottom row). Also note that domains of bright primary lamellar bone observed in CPL (bottom row, right) appear dark when observed parallel with the plane of extinction in LPL (top row, right). Images of bright and alternating osteons derive from modern human femoral midshaft, and images of the longitudinal osteon derive from the femoral midshaft of a brown-headed spider monkey (*Ateles fusciceps*). Field width of each frame = 475 μm .

polarized light microscopy of bone, is the same at any specific collagen fiber orientation within or between taxa.

Polarizing Light Microscopy of Bone

The examination of preferentially distributed collagen fibers within whole cross-sections of long bones, including domains occupied by secondary osteonal as well as all other tissue types (e.g., parallel fibered, circumferential lamellar, cancellous), was first attempted by Portigliatti-Barbos et al.

(1983). Images of 100- μm -thick sections obtained from the mid-shaft region of the human femur with linearly polarized light (LPL) suggested to these authors that the patterned distribution of preferentially oriented collagen was consistent with published strain data on the femur. See Box 1 for a brief description of linearly polarized light.

LPL images of transverse lamellae normally appear bright in comparison to the extinction of light from domains occupied by longitudinally oriented collagen fibers. However, wherever trans-

verse lamellae circle around 90 degrees of arc or more (e.g., circumferentially around the bone cortex or an individual osteon), reduced intensity of light occurs in the vicinity of each ± 45 degrees and ± 135 degrees rotational position relative to transmission axis of the polarizer (Figure 1b, top row). This finding creates a dark “Maltese Cross” effect against a bright background because the analyzer and polarizer filter transmission axes lie outside the vibration plane of light passing through lamellae at these positions. This artifactual reduction in intensity of brightness associated with transverse fibers interferes with one’s ability to appropriately measure, interpret, and relate pixel intensities to the proportion of transversely oriented collagen in a histological section (effectively increasing the perceived proportion of longitudinal lamellae). Circularly polarized light (CPL) eliminates the Maltese Cross artifact (Figure 1b, bottom row), presenting a correct polarized light image at any 360 degrees rotational position of the specimen.

The arrangement of filters required for CPL imaging is depicted in Figure 2. The transmission axes of polarizer and analyzer linear polarizing filters are crossed to provide background extinction. Between each linear polarizing filter and the specimen is a retarding quarter wave plate whose transmission axes (referred to as fast and slow) are oriented 45 degrees to their respective polarizer and analyzer axes (i.e., slow and fast axes at 45–225 degrees and 135–315 degrees, respectively). Quarter wave plates are crossed in subtractive position to restore background extinction. Let us examine CPL more closely.

Linearly polarized light, which is all in phase, becomes polarized into helical vibration planes when passing through a quarter wave retarder, or plate (Figure 2). A quarter wave plate has two transmission axes at 90 degrees to one another: fast and slow. Although these axes do not diminish the intensity of incoming polarized light, they do resolve the beam into two emerging orthogonal components: one along the fast axis and one along the slow axis when the incident polarized light lies between them at 45 degrees. Linearly polarized light resolved by the quarter wave plate along

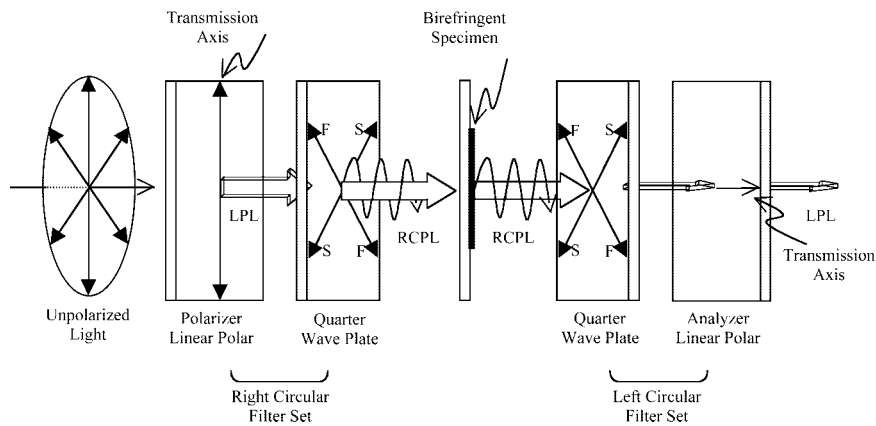


Figure 2. Diagram of a transmitted light circularly polarizing filter arrangement. The lamp source generates unpolarized light having vibration planes in all 360 degrees. This light is first converted into linearly polarized light (LPL) along the transmission axis of the polarizer and then bent into right circularly polarized light (RCPL) waves (clockwise to the observer) in the direction from fast (F) to slow (S) axes of the quarter wave plate filter. As circularly polarized light passes through a birefringent specimen, light is refracted in all 360 degree rotational positions. Refracted light is re-linearly polarized 90 degrees to the polarizer at the left circular quarter wave plate filter (having a 90-degree offset of F and S axes from that of the right circular quarter wave plate filter), which is then allowed to pass along the transmission axis of the analyzer. The emerging LPL is observed at the eyepiece objectives or the recording system.

the slow axis lags that of the fast axis and emerges from the filter one quarter wave length behind and out of phase; the light is no longer linearly polarized. The net vector of each component now vibrates around an elliptical axis, originally turned toward the slow axis to produce a right circular trajectory (clockwise toward the observer). This is CPL.

CPL will refract through a birefringent material such that its elements oriented parallel with the plane of section will transmit peak light intensities irrespective of their 360 degrees rotational position. Light emerging from the specimen maintains a right circular trajectory, but is then converted back into LPL by a second quarter wave plate whose fast and slow axes are reversed (extinction position) from the first. The LPL polarization sense is shifted 90 degrees owing to birefringence of the collagen fibers, aligning with the transmission axis of the analyzer.

Unlike LPL images of circumferential lamellae (Figure 1b, top row), lamellae containing collagen with a strongly oriented fibrillar component parallel with the plane of section appear bright in their entirety irrespective of their rotational position when imaged in CPL (Figure 1b, bottom row); each 45 degrees, 135 degrees, 225 degrees, and 315 degrees artifac-

tual reduction in LPL intensity is now occupied by quarter wave plate transmission axes (Figure 2). Light intensity, stemming from birefringence in an imaging system configured to provide CPL, varies with collagen fiber orientation at angles between 0 and 90 degrees from plane with the section, and this having been calibrated, permits one to quantify pixel intensity as it varies with fiber orientation (Riggs et al., 1993a).

To address the uncertainties associated with the quantitation of brightness in LPL images of bone, Boyde et al. (1984) developed an automated technique using CPL for examining the distribution of preferentially oriented collagen fibers. This permitted Portigliatti-Barbos et al. (1984) to subsequently map their distribution more accurately in a series of histological sections taken along the lengths of shafts from two human femora. Quantitative analyses of CPL images were improved by Boyde and Riggs (1990) who presented a simplified, rapid method for mapping preferential collagen fiber orientation patterns in whole cross-sections. Images captured at low magnification, using a macro lens and large circularly polarizing light filters, were visualized and quantified by color-coding grey-level bins. Several studies subsequently used this method to quantify the dis-

tribution of preferentially oriented collagen and to relate such distributions to existing bone strain data. Studies of the horse radius (Boyde and Riggs, 1990; Mason et al., 1995; Riggs et al., 1993a,b); the macaque circumorbital region (Bromage, 1992); and the calcanei of horse, sheep, and elk (Skedros et al., 1997) helped to support existing hypotheses of the relationship between preferred collagen fiber orientation and mechanical loading. Martin and Ishida (1989), Martin and Boardman (1993), and Riggs et al. (1993b) examined several material properties of bone and determined that collagen fiber orientation made the most significant contribution to the overall strength of bone tissue. McMahon et al. (1995) presented data from the sheep calcaneus, suggesting this relationship might be more complex than previously thought: the authors propose that low levels of localized tension may have a more significant impact on collagen fiber distribution than higher levels of peak compression in regions of some bone elements.

Because of the tremendous potential for CPL investigations of collagen fiber orientation in bone, we provide a detailed description of the sample preparation and imaging considerations required for its effective and quantitative evaluation. We subsequently describe a grey-level standard derived from femoral turkey tendon, which is potentially useful for quantitative CPL.

METHODOLOGICAL CONSIDERATIONS

Bone exhibits positive form birefringence dominated by and dependent upon the orientation of its collagen (see Box 1). Evaluation of the extent to which collagen is preferentially oriented and, by proxy, mineral crystallite orientation as well (Francillon-Vieillot et al., 1991, and references contained therein; Bonucci, 1984) within histological thin sections thus depends largely upon the intensity of circularly polarized light detected by the recording system (small contributions in light intensity may arise from variations in histocompositional variables such as mineralization density, but their significance remains unex-

Box 2: Additional Bone Cleaning Procedures and Details of Histological Preparation

Enhanced cleaning procedures. If cleaning proves difficult, this method may be modified by making up the Terg-a-Zyme solution in a 1% detergent solution of Tween 80 (Fisher Scientific, NJ), which enhances the solubility of the nonmineralized proteins. Because one's work may include an interest in bone mineral density, it is important that this cocktail be buffered by the alkaline Terg-a-Zyme. As the enzyme portion of the cocktail becomes less effective with time, we add additional enzyme at 24-h intervals, changing the cocktail itself every 72 h (the viscosity may increase over several days, and we reason that its effectiveness within the bone porosity diminishes). Bone specimens submerged in this cocktail are ultrasonicated for 10–15 min at each of the 24 and 72 h changes. It should be emphasized that this modification must only be tried on very-difficult-to-clean and robust spec-

imens. Samples need to be checked periodically for specimen degradation when Tween is used, as it more aggressively denatures all available nonmineralized proteins, some of which maintain the integrity of the bone during thin-section processing.

Histological section preparation. Our histological section preparation is briefly described here. Embedded bone blocks are ground to the section level using a graded series (240 to 1,200) of silicone carbide grit papers on a Handimet-2 (Buehler, IL). Glass slides are acid etched and treated with Porcelain Primer (Bisco, IL). Bone blocks, polished face down, are dipped into a ca. 1-mm film of acetonitrile for up to 5 min, depending on block size, and subsequently treated with a Dentine Activator (Parkell, NY). Blocks are brushed with a 50:50 solution of Prime & Bond NT and Self Cure Activator primers (Dentsply, IL)

and light cured. Blocks are then pressed to the slide in a film of Pro-bond adhesive (Dentsply, IL) and polymerized for 1–2 min by using a visible light curing gun. Mounted blocks are sawn away from the slide by using a Buehler Isomet or Petro-Thin, resulting in a ca. 150- μ m-thick embedded mounted sections. For transmitted light investigations of bone samples, the surface of the sections should be ground on silicone carbide papers to a final 1,200 grit, as described above. Sometimes we polish the surface to 1.0- μ m diamond on a Buehler Ecomet-3 (surface topography is not equivalent to the final polishing, as polishing surface fabrics produce negative relief in areas of less mineralization density). For imaging, sections must be cover-slipped with a nonaqueous solution (e.g., ethylene glycol) to improve image clarity (Goldman et al., 1999).

pored). However, the pixel intensity and, thus, the quantitative recording of grey-level information is conspicuously affected by four parameters: (1) section transparency, (2) section thickness, (3) the uniformity of the illuminating system, and (4) CPL paraphernalia.

These parameters form a yardstick against which quantitative investigations of preferred collagen fiber orientation in bone may be evaluated. While it is often, if not usually, the case that such conditions are difficult to realize, the extent to which any particular bone sample departs from these criteria should be evaluated on a case-by-case basis and noted. The methodological considerations described here pertain to the preparation and imaging of mineralized ground sections.

Section Transparency

It is necessary for bone thin sections to be clean of nonmineralized organic tissues (e.g., cells and their contents, vascular wall debris, fat, etc.) and other contaminants. This necessity is due to light scattering artifact occurring as background image "noise" in-

cluded with the birefringent signal from the bone. Typically, the bone itself, or a block derived from the bone, is cleaned. In the case when a bone block resists attempts to be cleaned (e.g., formalin-fixed tissue), the histological sections themselves may also have to be cleaned (see also Box 2).

We have had consistently excellent results using the technique of Boyde (1984), in which bone specimens are subject to regular changes of fresh 1% Terg-a-Zyme (Alconox, NY) enzyme solution at 50°C until cleaned (typically 1 to 2 weeks, depending on the size and previous storage conditions of the sample). Bone specimens may be prepared in the absence of a 50°C oven, but enzymatic activity is less efficient and more time will be required. One need not worry about mineralized collagen degradation at 50°C, this occurring only at much higher temperatures (150°C; Wang et al., 2001).

Ground sections may be mounted in water alone or with a hydrophilic mounting medium. In this case, dehydration is unnecessary and specimen transparency is good. In our work, bone specimens are dehydrated because our embedding and mounting

media are hydrophobic. Residual water in this case can result in less than ideal media infiltration, leading to light scattering effects independent of the bone structure. After enzyme-detergent treatment, bone specimens are subject to rigorous ethanol substitution (using graded ethanol:H₂O changes at proportions of 50:50, 70:30, 95:5, and 100:0) with 5-min ultrasonication and vacuuming at each change. The time required for these changes will range from 24 h in the case of relatively large bone blocks to 10–15 min in the case of an already prepared but unembedded and unmounted thin section.

Fat may be removed from bone specimens when found to inhibit penetration and proper curing of embedding and mounting media. Bone blocks are subject to 50:50 isopropanol:heptane and reflux in this solution for 7–14 days in a Soxhlet apparatus, the amount of time varying in respect to small and large bone blocks respectively (Goldman et al., 1999). Any remaining free water, as well as the fat, is washed out of the bone round-the-clock using this method. Bone blocks may be prepared in the absence of a

Soxhlet apparatus with daily changes of 50:50 isopropanol:heptane, but more time, chemicals, and ultrasonication may be required to defat the bone. Bone thin sections may also be subjected to the isopropanol:heptane without refluxing but with several changes of fresh solution over several hours, days, or more, depending on an inspection of any remaining fat.

Section Thickness

A 100- \pm 5- μ m ground section thickness has been a standard in collagen fiber orientation studies (e.g., Boyde and Riggs, 1990; Portigliatti-Barbos et al., 1984). Uniform section thickness is critical for the quantitative analysis of collagen fiber orientation. Differential brightness within and between specimens may be purely a result of the optical path difference through which light passes through the section, rather than an indication of fiber orientation (Boyde et al., 1984).

When possible, grinding and polishing should be undertaken on mounted (cemented to a glass slide) sections. This method has the advantage of providing a highly uniform section thickness. The procedure of Goldman et al. (1999), results in the firm adhesion of the section to the slide during all grinding and polishing procedures (see Box 2).

The preparation of unmounted 100- \pm 5- μ m-thick bone sections specimens is also possible with a variety of technologies (e.g., a Leitz annular saw; Boyde and Riggs, 1990). Such sections, particularly from unembedded bone blocks, can be obtained without sophisticated sectioning and grinding technologies, but care must be exercised to ensure the even removal of material, rendering a uniform section thickness. It is nearly always the case that plane-parallel unmounted sections must be ground between flat platforms. The mounting of these thin sections is easily undertaken with conventional light microscopy mounting media, as the mounting medium has not to withstand grinding and polishing procedures noted above.

As the uniformity of section thickness is important, so is the care that must be exercised in their measurement. Measurements must be made at

intervals around the section at a density sufficient to ensure section uniformity within the \pm 5- μ m standard. In our laboratory, we are able to measure section thickness to \pm 2 μ m by using an Edge R400 real-time three-dimensional microscope fitted with factory calibrated precision staging in the "Z" direction. Our experience with this optical, noncontact measurement technique has demonstrated to us that measurements made with a grade of hand micrometer conventionally used for determining section thickness (e.g., 10- μ m interval micrometer) are frequently on the order of \pm 10 μ m away from our optical measurements (even when achieving excellent precision). This, we believe, is due primarily to microscopic debris distributed on the section, the micrometer tips, or both, and/or very small variations in the timing, speed, and pressure applied to the micrometer spindle. We can attest to greater than 10- μ m-diameter particles in New York tap water, so rinsing in distilled water or some other particulate-free solution is also a variable to consider before measurement. Thus attention to section cleanliness, dynamic variables, repeatability, and perhaps measurement averaging are extremely important when using these instruments. Digital micrometers will improve the reliability of measurements, but considerable care in their operation is still warranted.

Finally, we wish to emphasize that *uniformity* in section thickness is more critical than section thickness itself. The 100- \pm 5- μ m-thick section became standard in many laboratories as a compromise between being thin enough to limit out of focus planes at moderate magnification but thick enough for some extended range imaging potential and ease of handling (the latter especially during manual preparation procedures). It is obvious that, as section thickness diminishes, the contributions that voids make to the average brightness, for instance, will increasingly relate to background intensities and be eliminated from measurements of collagen fiber orientation. Should there, say, be significant species-specific differences in the proportions of voids having an influence on average brightness, then some image analytical or preparation

accommodations would have to be made when making comparisons between taxa. This aspect is an important area for future research.

Uniformity of the Illuminating System

The illuminating system is often the least understood component of the microscope, and is frequently the cause of variability in brightness equal to or exceeding either of the two parameters described above. Because variation in brightness has to be related only to collagen fiber orientation under ideal conditions, the researcher must consider any deviations in brightness across the field of view which may be due to nonuniform illuminating conditions.

Most microscopes today are constructed such that the illuminating system is either permanently aligned at the factory or may be easily aligned when, for various reasons, components are shifted about the optical axis relative to each other. Before imaging, the microscope should be set up to provide Koehler illumination, as this method is designed to image the lamp source at the aperture rather than the specimen, rendering as even an illuminating background across the field of view as can be obtained with the microscope. Evenness of the illuminated field of view is further improved if the lamp condenser is frosted, thus diffusing the effects of lens aberrations.

However, despite all conditions being optimized, it is sometimes the case that the illumination is uneven across the field of view. It would be difficult to know this if it were not for the advent of digital image recording systems capable of discriminating levels of grey along a wide dynamic range. Good quality monochrome CCD cameras record significant grey-level differences otherwise beyond the capability of the human visual system. (In the absence of a monochrome camera, it is possible to acquire standardized CPL images if the maximum and minimum intensity thresholds can be set using a single color band; see Box 3). Thus, although we may visually interpret the field of view to be even, it sometimes is not.

To compensate for nonuniformity

Box 3: Color Cameras and Analytical Standards Compared

Image acquisition using a color CCD camera. When using a three-chip (RGB) CCD color camera, light contributions from the red and blue bands can be effectively eliminated with a narrow band-pass green filter (e.g., we use a filter, which transmits maximally at 546 nm, has a half band width of approximately 15 nm, and whose maximum transmission is approximately 40%). With an RGB color camera, the green band is best used for grey-level imaging; peak quantum efficiency of most monochrome cameras more closely resembles that of the green portion of the visible light spectrum than those portions occupied by red or blue. In addition, a narrow-band green filter effectively eliminates red and blue CPL artifact arising from a retardation difference between quarter wave filters.

Standardization methods. Standardization methods, such as the use of the Longitudinal Structure Index (LSI) introduced by Martin and Ischida (1989) may allow for greater comparability between samples, but

still they do not permit interlaboratory comparisons of average grey values. The LSI represents a ratio obtained by dividing the brightfield by the dark-field measurement. By using the LSI, the authors argued that the effects of staining and porosity on light intensity could be corrected (Martin and Ischida, 1989). Takano et al. (1999) extended this method by normalizing results to attempt to correct for differences in section thickness and staining. These studies focused not on global patterning at a macro level but rather on small sample areas taken from different cortices of the bone.

The method used by Boyde and Riggs (1990) for quantifying collagen fiber orientation differs from the LSI in an important way. The Boyde and Riggs (1990) method takes into account the variability in the entire grey-level spectrum, providing a measure of both average grey values, as well as the distribution of values within the entire grey-level range. The LSI, on the other hand, provides only a mea-

sure of longitudinal lamellae and does not allow the distribution of grey values over the entire spectrum to be analyzed. Further to this, one of the assumptions of the LSI is that pores appear brighter than longitudinal lamellae in polarized light and, therefore, are not included in the calculation of LSI. In practice, it is difficult to distinguish pores from longitudinal lamellae by their grey-level values. In such a situation, the LSI would not provide an accurate assessment of longitudinal lamellae. Therefore, it was determined that the adaptation of the method used by Boyde and Riggs (1990) and Riggs et al. (1993a), with the addition of background masks to eliminate the effect of large pores, would provide a more appropriate measure of collagen fiber orientation (images are masked with a transmitted light image of the same field of view and background, large pores, and resorption spaces in the CPL image are assigned a grey level of 0; cf. Goldman et al., 2003).

of the illuminating system, background, or shading, correction must be performed by using image processing functions available in most image analyzing systems. During this correction, the grey levels of all pixels in the array are recorded from a blank field (normally a field of view at the periphery of the section), pixel statistics are derived from the array, and deviations from the mean at all pixels are calculated. Interpolated grey-level corrections are then reassigned for each pixel in the array. This algorithm is stored and subsequently applied to all images acquired by the recording system. We have observed that it is necessary to check the correction algorithm periodically for any specific lens configuration, because as a lamp filament ages, the illumination characteristics of the system also tend to change.

CPL Paraphernalia and Setup

The filter setup in CPL depends on whether polarizing and quarter wave plate filters are prealigned and sand-

wiched into right and left circular polars, or whether separate filters must each be positioned (Figure 2). In the case of right and left circular polars, such as we use on our macro imaging devices, the filters are rotated until maximum background extinction occurs. This position can be checked by the image recording and processing system in real time using lower limit thresholding. If individual polarizing and quarter wave plate filters are used, then polarizer and analyzer are first aligned to provide maximum background extinction in a blank field. Quarter wave plate filters are then positioned, one above the objective and the other below the specimen. In most compound microscopes, a 45 degree compensator slot facilitates its alignment, while the quarter wave plate below can be rotated. Alignment of the lower quarter wave plate to achieve background extinction may be performed in real time, as described above. (Alternately, increase the illumination above normal CPL imaging conditions and rotate the

lower quarter wave plate until the deepest magenta is perceived through the eyepiece objectives.)

The best CPL will be obtained when the quarter wave filters have been cut to the same thickness and derived from the same piece of material, because if they are not homogeneous, or are of different thickness, color and linear polarizing artifacts will occur owing to their differential retarding of the light. It is generally observed that differences between quarter wave filters of only 1- to 5-nm retardation are relatively inconsequential, but that differences greater than this increasingly manifest visible polarizing artifacts. If a CPL artifact due to differences in retardation is evident, one solution is to obtain several filter sets and mix and match until you have the best CPL. For instance, with cooperation from Leica Microsystems, Inc., we compared off-the-shelf quarter wave plates until a pair measuring 131.6- and 135.4-nm retardation were identified. Although minor extinction artifact is still occasionally observed,

the retardation difference of only 3.8 nm provides satisfactory results obtainable from readily available filter stock. We hasten to mention, however, that quantitative CPL imagery is possible with inexpensive but reasonably uniform quarter wave plate or circular polar filter material available from commercial optical supply houses. With such filters, care needs to be taken to ensure that they are held flat, as some filters exhibit curvature, causing image distortion.

If there is reason to believe that observed CPL artifacts are not due to filter alignment and quality, it may be that strain-free objectives designed for polarized light imaging are required. If only the acquired images exhibit artifact, it is possible that the CCD adapter-reducing lens is not strain-free.

QUANTITATIVE CPL STANDARD

To date, CPL illumination standards have been laboratory specific. Although results are internally quantitative, comparisons of samples produced across laboratories have emphasized qualitative appreciations of patterned preferentially oriented collagen fiber domains within bone thin sections. This qualitative emphasis has provided functionally important information on several skeletal elements and taxa. However, it may not readily permit quantitative comparisons of results obtained between laboratories. See Box 3 for a discussion of other standardization methods.

For many years, our laboratory has used neutral density filters to standardize imaging conditions. Study specimens are observed whilst adjusting the illumination until the full dynamic range is represented: peak pixel intensities near to a grey level of 255 in regions of transverse fibers and background intensities rendered near to a grey level of 0 in regions of longitudinal fibers. A neutral density filter is then placed in the optical path, and the grey level is read. All subsequent imaging of study sections in the sample is based on a neutral density filter setup procedure in which these illuminating conditions are re-established to obtain this grey-level value.

Because this method depends on

imaging setup conditions relevant to the sample under investigation, that is, possible differences between taxa and instrumentally determined grey-level thresholds by individual laboratories, our ability to make quantitative interlaboratory comparisons is compromised. For instance, this method assumes the presence of some perfectly transverse fiber domains appearing maximally bright in every section, but such domains may not exist, setup conditions thus artificially raising the illumination to bring near-to-transverse domains up to peak pixel intensities.

We have begun to explore the usefulness of a standard based on mineralized turkey tendon. We chose turkey tendon as the standard because of several advantages. Type I collagen is the principle fibrillar protein of both bone

Investigations of collagen fiber orientation in bone by circularly polarized light microscopy provide important insights on the biomechanical efficacy of the skeleton.

and tendon (Rossert and de Crombrugge, 1996). Also, turkey tendon is readily available, a byproduct of the acquisition being available as lunch or dinner (for those of us on tight research budgets). The use of turkey tendon as a standard has another distinct advantage: While bone may have a complex arrangement of collagen fiber orientations, which we cannot easily know, turkey tendon is regarded as highly organized, having its collagen fibers parallel, or very nearly so, and along the tendon axis (Traub et al., 1992). Thus, the collagen orientation can be inferred to be reasonably well known and thus may be used as a standard with respect to similar orientations in bone thin sections.

Here, we describe our procedure for obtaining a CPL turkey tendon standard. Three fresh gastrocnemius tendons were obtained from supermarket

ca. 20-week (i.e., ca. 32-lb whole turkey) domestic farmed turkey legs, *Meleagris gallopavo*. After severing the mineralized insertion close to the bone, approximately 1-cm lengths of mineralized flat tendon, taken furthest from the mineralizing front (i.e., the most mineralized portion at its connection with the bone), were cut and prepared as described above for bone. Once cleaned, they were ground on one flat side with 1,200-grit silicone carbide grit papers and subject to the preparation procedures. Ground flat sides were mounted down into polymethyl methacrylate (PMMA), according to the method of Boyde (1984) and, once cured, the PMMA blocks were ground/polished to section level, mounted, ground, and polished to a thickness of $100 \pm 5 \mu\text{m}$.

Specimens were cover-slipped with ethylene glycol and observed on a Leica DMRXE (Wetzlar, Germany) compound microscope configured for CPL imaging as described above. The DMRXE lamp was run for at least 0.5 h before imaging to avoid instability during initial filament burn. The illumination was roughly adjusted until all but the extremes of the entire dynamic range were represented. Fine adjustments to lower and upper limit thresholds were made by DMRXE lamp and Leica Quantimet 550 (Q550; Cambridge, England) image setup controls until the background grey values equaled 5 and brightest grey values equaled 250 (5/250). Images of $100 \pm 5 \mu\text{m}$ bone thin sections were subsequently acquired with an Adimec MX12P monochrome camera (Eindhoven, The Netherlands) and transferred to the Q550 for grey-level measurement. Under these conditions, extended depth of focus three-dimensional imaging was also performed with the aid of Syncrosopy Auto-Montage software (Frederick, MD).

RESULTS

The fully calcified $100 \mu\text{m}$ turkey tendon preparations were surveyed in X and Y and at Z focal depths within each section (Figure 3). Each preparation contained brightest foci, which, when adjustments were made to achieve 5/250 imaging conditions for one preparation, closely matched the imaging conditions of the others (i.e.,

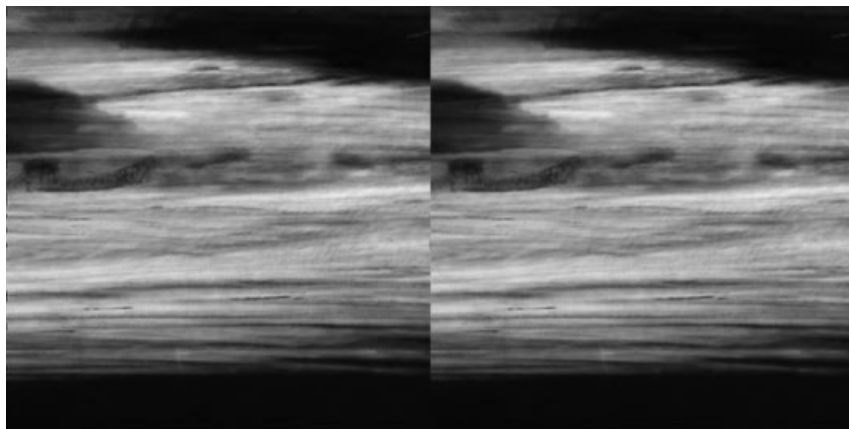


Figure 3. Stereopair of 100- μm -thick section of mineralized turkey tendon (5/250). In this slip of tendon, note the void at upper left and, beneath this, a blood vessel channel coursing from left to right. A three-dimensional view may be obtained with a stereo viewer or by mental reconstruction of left and right images into one stereoscopic image. Field width of each frame = 600 μm .

within ± 2 grey levels in each of the 5 and 250 grey-level values).

A 100- μm ground section derived from the slow loris (*Nycticebus coucang*) humerus was subsequently observed at 5/250 imaging conditions established on the 100- μm turkey tendon. Pixel intensities varied in the range 2/232 (Figure 4), rendering an image, which we regard as both visually appropriate and quantitatively comparable to other study sections imaged in the same way.

The image of mineralized tendon (Figure 3) will be observed to be rather different from an image of bone at the same magnification (Figure 4). Tendon collagen fibers are imaged in their transverse orientation, thus the entire field of view may be likened to pixel intensities representative of transverse lamellae in bone, but without lamellar structure. Furthermore, the image of bone is punctuated by dark primary and secondary osteons in the midst of bright circumferential lamellae (Figure 4).

Stereoscopic examination of the tendon reveals that variation in grey level is due to collagen fiber orientations out-of-parallel with the plane of section and to voids (e.g., vascular canals), which effectively reduces the path difference at locations not containing mineralized tendon through the full thickness of the section (Figure 3).

DISCUSSION

Investigations of collagen fiber orientation in bone by circularly polarized

light microscopy provide important insights on the biomechanical efficacy of the skeleton, particularly with respect to studies of functional and ecological morphology. Given the potential for many useful and innovative variations in specimen preparation and imaging by our research community, it was our primary intention here to emphasize those methodological considerations critical to the effective performance of a robust technique for achieving comparable quantitative results observed across specimens and within and between taxa, investigators, and laboratories.

Here, we provide examples drawn from the nonhuman primate and hu-

man skeleton. To visualize the quantitative results, CPL images have been subject to a color look-up-table (LUT) which, here, divides the 256 grey-level scale into eight equal "bins" and assigns a unique color to each. The LUT is expressed according to the color scheme represented on the Figure 5 color plate. Reds and grey in the colorized image represent increasingly transversely oriented collagen fibers (bright in CPL), and increasingly longitudinally oriented collagen fibers (dark in CPL) are represented by green and deepening shades of blue (Figure 5a–c).

Slow Loris Midshaft Humerus

Unique among primates, loris locomotion is characterized by a stealthy, sure-footed, and flexible movement through the trees, with an absence of leaping (Figure 5a). The limbs are used in an acrobatic manner as members of this group navigate deliberately above and below branches, accommodating a range of support geometries. A slow loris (*Nycticebus coucang*) 100- μm -thick midshaft humerus section was observed at 5/250 imaging conditions established on the 100- μm turkey tendon (as it was also in Figure 4). A predominance of longitudinal collagen fibers, appearing dark in CPL, is discerned for both primary bone tissues, as well as the fibers making up the secondary osteons, or remodeled bone. This predominantly

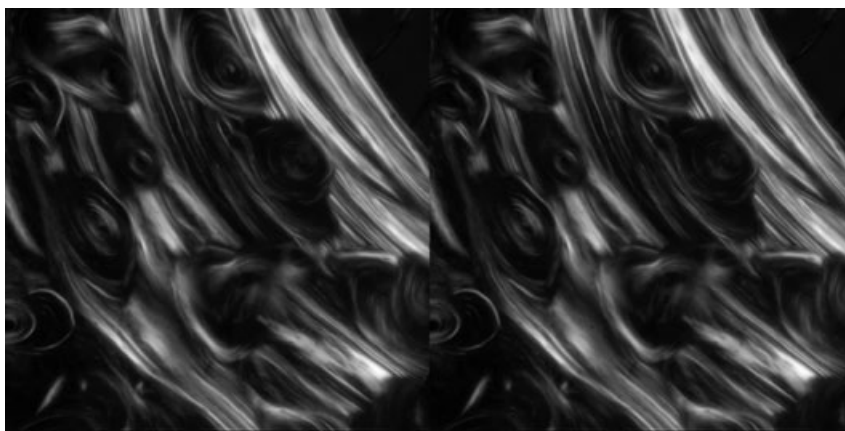


Figure 4. Stereopair of 100- μm slow loris (*Nycticebus coucang*) humerus (having minimum and maximum grey levels of 2/232) assessed with illumination conditions established on a 100- μm -thick section of mineralized turkey tendon (minimum and maximum grey levels of 5/250). A three-dimensional view may be obtained with a stereo viewer or by mental reconstruction of left and right images into one stereoscopic image. Field width of each frame = 600 μm .

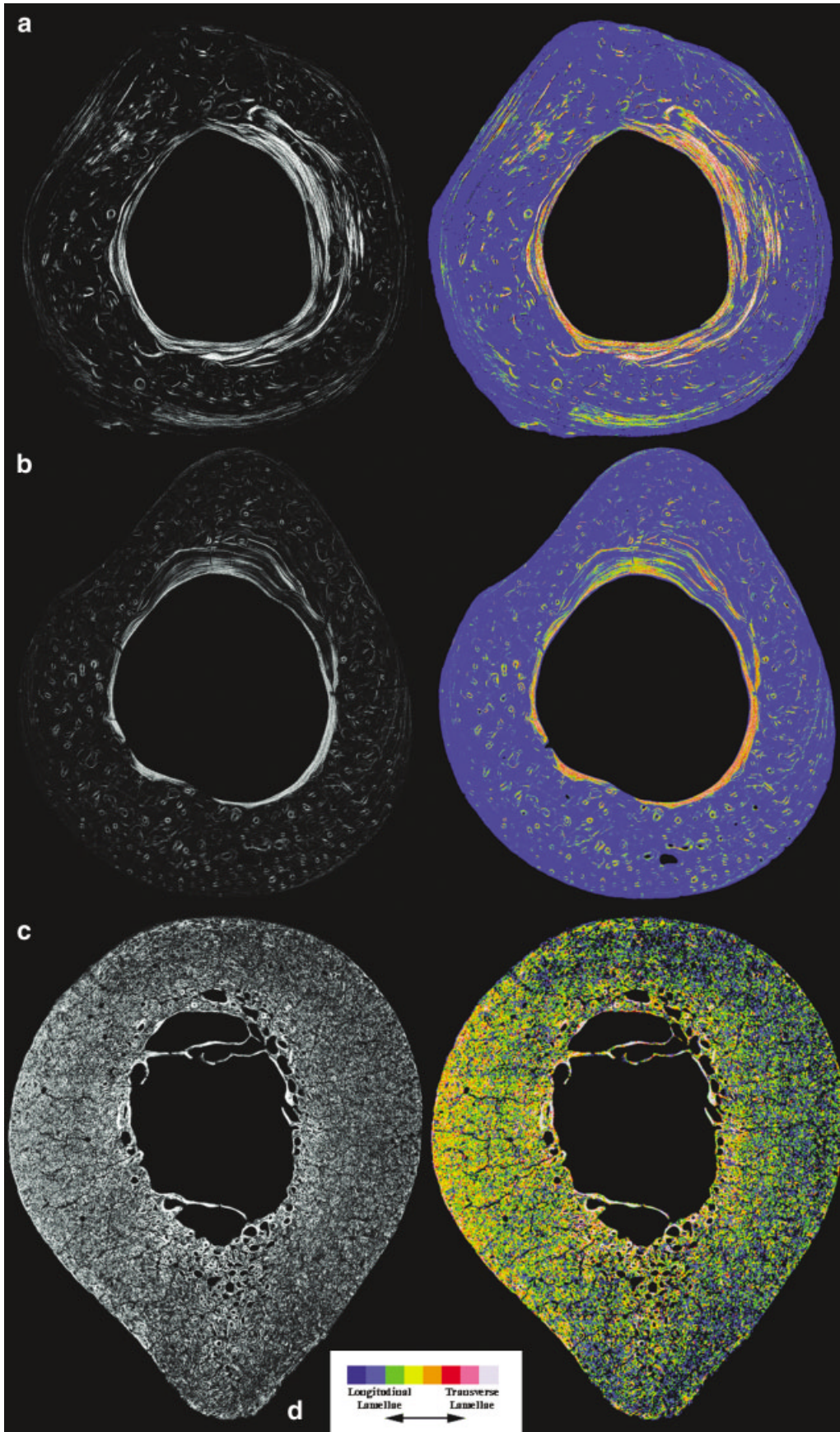


Figure 5. Examples drawn from our nonhuman primate and human circularly polarized light (CPL) imaging research include macroscopic images of 100 ± 5 - μm -thick sections of the midshaft humerus of the slow loris (*Nycticebus coucang*; **a**), the midshaft ulna of a gibbon (*Hylobates lar*; **b**), and the midshaft femur of a human (*Homo sapiens*; **c**). For each, at left is the grey-level CPL image according to illumination conditions established on the mineralized turkey tendon standard, and at right, to appreciate the quantitative results, the pseudocolor image generated by dividing the grey-level dynamic range (0, black to 255, white) into eight-color intervals of 32 levels each by using a thermal color scheme (**d**). Sections are presented with anterior at top and medial at left. The slow loris humerus (**a**, section width = 4.7 mm) and gibbon ulna (**b**, section width = 6.8 mm) are composed mostly of lamellae containing longitudinally oriented collagen fibers and appearing blue in the colorized image. However, note the bright transversely oriented collagen fibers along the endosteal (inner, or medullary) margin of each bone, represented in shades of orange, red, pink, and grey. The human femur (**c**, section width = 26.4 mm) is composed variously of lamellae containing transversely and longitudinally oriented collagen fibers. However, note that relatively more transversely oriented collagen fibers, appearing in shades of orange and pink, increase along the endosteal margin of the bone and along the medial femoral cortex.

dark signal also matches that found in the femur of the same animal. By contrast, in many other primates (e.g., the leaping bushbabies), the humerus displays increased brightness overall relative to the femur. Although further studies are required, which would determine the actual loads experienced at the midshaft, the distinctive pattern seen in this loris humerus, repeated in both primary and secondary tissue, provides evidence that bone collagen deposition may conform to species-specific patterns of loading.

Gibbon Midshaft Ulna

Gibbons practice a highly specialized form of suspensory locomotion termed brachiation (Figure 5b). During brachiation, the animal's body mass is supported entirely by the forelimbs, which grasp an overhead support as the animal swings from branch to branch in a pendular motion. In vivo strain gauge analysis demonstrates that during brachiation, the gibbon ulna is loaded predominantly in axial tension (Swartz et al., 1989). A gibbon (*Hylobates lar*) 100- μ m-thick midshaft ulna section was observed at 5/250 imaging conditions established on the 100- μ m turkey tendon. In this element, collagen is deposited with a preferred longitudinal orientation in both primary tissues deposited during growth and in secondarily remodeled bone. As described above, it has been hypothesized that longitudinally oriented collagen is adapted to withstand tensile strains. This finding provides further confirmation that axial tensile loads are the predominant loading regimen experienced by this element in the gibbon.

The above examples represent first glimpses of preferential collagen fiber orientations in nonhuman primate bone. This exploration is hoped to extend to a variety of primates in future research. To date, our research on human femoral collagen fiber orientations is well under way.

Human Midshaft Femur

The human femur is subject to a variety of axial and compound forces during the various stages of bipedal locomotion (Figure 5c). At the mid-shaft,

bending forces may be particularly high during single leg support stance, with the anterior and anterolateral aspects of the cortex subject to tension and the posteromedial and medial aspects subject to compression. The linea aspera, as a muscle attachment site, experiences predominantly tensile forces. This CPL image of a cross-section of the mid-shaft femur of a 27-year-old urban Australian female demonstrates a distribution of preferred collagen fiber orientation in which transversely oriented collagen fibers predominate in areas corresponding to high compression, whereas longitudinal collagen fibers predominate in areas corresponding to high tension. Although this relationship between collagen fiber orientation and bending stresses agrees well with our understanding of the bending forces in the human femur, research on a larger urban Melbourne autopsy sample ($n = 67$) has shown that a tremendous amount of variation exists in this pattern among adults (Goldman et al., 2003). In this study, although collagen fiber orientation appears nonrandomly distributed across the mid-shaft femur sample, no single "human" pattern was identified. However, differences between age and sex groups suggest a correspondence between collagen fiber orientation and tissue type distributions. The myriad factors that may influence collagen fiber orientation patterning, including growth trajectories, metabolic and nutritional status, and disease states, need to be explored further. Only then, in conjunction with studies of other structural and material properties of bone, will we elucidate the linkages between microstructure and functional adaptation at the human mid-shaft femur.

We wish to note here that the human femur section was originally imaged according to neutral density filter setup conditions described above (quantitative CPL standard). Our goal in this instance, however, was to obtain an image corrected to 5/250 imaging conditions established on the 100- μ m turkey tendon. To do this, we established imaging conditions for the neutral density filter setup until the specified grey value for that study was achieved and noted. We then imaged the 100- μ m turkey tendon standard

until 5/250 conditions were realized. The turkey tendon standard was removed and the neutral density filter placed back into the light path and imaged. The grey value was recorded, which, in this instance, was below that of the original setup conditions, and the difference in grey values was noted. This difference in grey values was subtracted from all pixel intensities of the image histogram in Adobe Photoshop (San Jose, CA) after which the image was squeezed from only the dark extreme to bring black levels back to the value 5. This procedure generates a histogram correction, which may then be reasonably applied to archived images within the study.

Not all study samples are readily amenable to quantitative CPL examination. We have commonly observed, within modern fresh and archived skeletal samples (e.g., autopsy, cadaver, and museum collection specimens), variation in specimen preservation and preparation that make comparisons between individuals or between whole samples difficult. We encourage readers to consider nonhuman primate and human bone examples found in Kalmey and Lovejoy (2002), which helps to raise awareness of the need for researchers to evaluate these considerations when performing circularly polarized light investigations of collagen fiber orientation in bone. When factors affecting specimen heterogeneity and less than ideal imaging conditions occur, we must take care to scrutinize our results.

This brings us to describe the protocol by which investigators may contact us for a standard. We will calibrate 25-mm square neutral density filter material according to 5/250 imaging conditions established on the 100- μ m turkey tendon. The filter and its associated grey value will be provided on request. Alternately, investigators may provide us with their own neutral density filter in transmission percent ranges of approximately 40–60% (e.g., density 0.4–0.2), and we will calibrate this against 5/250 imaging conditions established on the 100- μ m turkey tendon. On using these standards, the illumination must be adjusted until the associated grey value is achieved. Background black levels must then be adjusted indepen-

dently to achieve the value 5 on a blank field at the periphery of the study section.

When attention to details of specimen preparation and imaging are properly applied, comparisons between specimens within laboratories provide useful results amenable to functional interpretation. These methodological considerations, taken together with the use of the turkey tendon/neutral density standard, permit comparisons between laboratories as well. In this way, a larger body of work can be accumulated to further our understanding of variation in preferred collagen fiber orientations in bone.

ACKNOWLEDGMENTS

We thank Jan Hinsch, Leica Microsystems, Inc., for his help in obtaining a calibrated CPL filter set for our microscope and for his comments on polarizing microscopy in general. Much appreciation is extended to the Leakey Foundation (General Grants 2001, 2002), the National Aeronautics and Space Administration (NAG5-6806), and the National Science Foundation (BCS-0079700, BCS-0202823, and BCS-0205185) for generous support of our hard tissue biology program. We also thank three anonymous reviewers for their critical and very useful comments.

LITERATURE CITED

- Ascenzi A, Benvenuti A. 1986. Orientation of collagen fibers at the boundary between two successive osteonic lamellae and its mechanical interpretation. *J Biomech* 19:455-463.
- Ascenzi A, Bonucci E. 1964. The ultimate tensile properties of single osteons. *Anat Rec* 158:160-183.
- Ascenzi A, Bonucci E. 1967. The tensile properties of single osteons. *Anat Rec* 158:375-386.
- Ascenzi A, Bonucci E. 1968. The compressive properties of single osteons. *Anat Rec* 161:377-392.
- Ascenzi M-G, Ascenzi A, Benvenuti A, Burghammer M, Panzavolta S, Bigi A. 2003. Structural differences between "dark" and "bright" isolated human osteonic lamellae. *J Struct Biol* 141:22-33.
- Bonucci E. 1984. The structural basis of calcification. In: Ruggeri A, Motta PM, editors. *Ultrastructure of the connective tissue matrix*. Boston: Martinus Nijhoff. p 165-191.
- Boyde A. 1984. Methodology of calcified tissue specimen preparation for SEM. In: Dickson GR, editor. *Methods of calcified tissue preparation*. Amsterdam: Elsevier. p 251-307.
- Boyde A, Riggs CM. 1990. The quantitative study of the orientation of collagen in compact bone slices. *Bone* 11:35-39.
- Boyde A, Bianco P, Portigliatti-Barbos M, Ascenzi A. 1984. Collagen orientation in compact bone. I. A new method for the determination of the proportion of collagen parallel to the plane of compact bone sections. *Metab Bone Dis Relat Res* 5:299-307.
- Bromage TG. 1992. Microstructural organization and biomechanics of the mastic circumorbital region. In: Smith P, Tchernov E, editors. *Structure, function and evolution of teeth*. London: Freund Publishing House. p 257-272.
- Francillon-Vieillot H, de Buffr nol V, Castanet J, et al. 1991. Microstructure and mineralization of vertebrate skeletal tissues. In: Carter JG, editor. *Skeletal biomineralization: Patterns, processes and evolutionary trends*. New York: Van Nostrand Reinhold. p 471-530.
- Gebhardt W. 1905.  ber funktionell wichtige Anordnungsweisen der feineren und gr oeren Bauelemente des Wirbeltierknochens. *Arch Entwickl Org* 20:187-322.
- Giraud-Guille MM. 1988. Twisted plywood architecture of collagen fibrils in human compact bone osteons. *Calcif Tissue Int* 42:167-180.
- Goldman HM, Kindsvater J, Bromage TG. 1999. Correlative light and backscattered electron microscopy of bone. I. Specimen preparation methods. *Scanning* 21:40-43.
- Goldman HM, Bromage TG, Thomas CDL, Clement JG. 2003. Preferred collagen fiber orientation at the human mid-shaft femur. *Anat Rec* 272A:434-445.
- Kalmey JK, Lovejoy CO. 2002. Collagen fiber orientation in the femoral necks of apes and humans: Do their histological structures reflect differences in locomotor loading? *Bone* 31:327-332.
- Marotti G. 1993. A new theory of bone lamellation. *Calcif Tissue Int* 53(Suppl 1):S47-S56.
- Martin RB, Boardman DL. 1993. The effects of collagen fiber orientation, porosity, density, and mineralization on bovine cortical bone bending properties. *J Biomech* 26:1047-1054.
- Martin RB, Ishida J. 1989. The relative effects of collagen fiber orientation, porosity, density, and mineralization on bone strength. *J Biomech* 22:419-426.
- Mason MW, Skedros JG, Bloebaum R. 1995. Evidence of strain-mode-related cortical adaptation in the diaphysis of the horse radius. *Bone* 17:229-237.
- McMahon JM, Boyde A, Bromage TG. 1995. Pattern of collagen fiber orientation in the ovine calcaneal shaft and its relation to locomotor induced strain. *Anat Rec* 242:147-158.
- Portigliatti-Barbos M, Bianco P, Ascenzi A. 1983. Distribution of osteonic and interstitial components in the human femoral shaft with reference to structure, calcification and mechanical properties. *Acta Anat* 115:178-186.
- Portigliatti-Barbos M, Bianco P, Ascenzi A, Boyde A. 1984. Collagen orientation in compact bone. II. Distribution of lamellae in the whole of the human femoral shaft with reference to its mechanical properties. *Metab Bone Dis Relat Res* 5:309-315.
- Riggs CM, Lanyon LE, Boyde A. 1993a. Functional associations between collagen fibre orientation and locomotor strain direction in cortical bone of the equine radius. *Anat Embryol (Berl)* 187:231-238.
- Riggs C, Vaughan L, Evans G, Lanyon L, Boyde A. 1993b. Mechanical implications of collagen fibre orientation in cortical bone of the equine radius. *Anat Embryol (Berl)* 187:239-248.
- Rho J-Y, Kuhn-Spearing L, Zioupos P. 1998. Mechanical properties and the hierarchical structure of bone. *Med Eng Phys* 20:92-102.
- Rossert J, de Crombrughe B. 1996. Type I collagen: Structure, synthesis, and regulation. In: Bilezikian JP, Raisz LG, Rodan GA, editors. *Principles of bone biology*. San Diego: Academic Press. p 127-142.
- Simkin A, Robin G. 1974. Fracture formation in differing collagen fiber pattern of compact bone. *J Biomech* 7:183-188.
- Skedros JG, Su SC, Bloebaum RD. 1997. Biomechanical implications of mineral content and microstructural variations in cortical bone of horse, elk, and sheep calcanei. *Anat Rec* 249:297-316.
- Swartz SM, Bertram JEA, Biewener AA. 1989. Telemetered in vivo strain analysis of locomotor mechanics of brachiating gibbons. *Nature* 342:270-272.
- Takano Y, Turner CH, Owan I, et al. 1999. Elastic anisotropy and collagen orientation of osteonal bone are dependent on the mechanical strain distribution. *J Orthop Res* 17:59-66.
- Traub W, Arad T, Weiner S. 1992. Growth of mineral crystals in turkey tendon collagen fibers. *Connect Tiss Res* 28:99-111.
- Wang X, Li X, Yamashita J, Agrawal CM. 2001. A novel method for quantifying normal collagen molecules in non calcified and calcified collagen in bone. *Proceedings of the Orthopaedic Research Society*, February 25-28, 2001: 0470.